Calculation

Mater. Res. Soc. Symp. Proc. Vol. 1352 © 2011 Materials Research Society
DOI: 10.1557/opl.2011.1007

First-principles study of Oxygen deficiency in rutile Titanium Dioxide

Hsin-Yi Lee,[1] Stewart J. Clark,[2] John Robertson[1]
[1]Engineering Department, Cambridge University, Cambridge, CB2 1PZ, UK
[2]Physics Department, Durham University, Durham, DH1 3LE, UK

ABSTRACT

The energy levels of the different charge states of an oxygen vacancy and titanium interstitial in rutile TiO_2 were calculated using the screened exchange (sX) hybrid functional [1]. The sX method gives 3.1 eV for the band gap of rutile TiO_2, which is close to the experimental value. We report the defect formation energy of the oxygen deficient structure. It is found that the defect formation energies, for the neutral charge state, of oxygen vacancy and titanium interstitial are quite similar, 2.40 eV and 2.45 eV respectively, for an oxygen chemical potential of the O-poor condition. The similar size of these two calculated energies indicates that both are a cause of oxygen deficiency, as observed experimentally [2]. The transition energy level of oxygen vacancy lies within the band gap, corresponding to the electrons located at adjacent titanium sites. The sX method gives a correct description of the localization of defect charge densities, which is not the case for GGA [3-6].

INTRODUCTION

Titanium dioxide (TiO_2) is a widely used material ranging from a substance used in solar cells, photocatalysts and nano-scale electronic devices. It has received a great deal of attention because it possesses many useful properties, such as high dielectric constant, good chemical stability, low cost and high refractive index [7]. Understanding the electronic and structural properties of the bulk and defective structures of TiO_2 is essential to improve the practical applications.

There are three different polymorphs of TiO_2 in nature: rutile, anatase, and brookite. Out of the three phases, the rutile is the most abundant naturally occurring phase and is the stable state under atmospheric conditions [3], hence it has been chosen as the major subject of this work.

Figure 1 shows the crystal structure of rutile TiO_2.

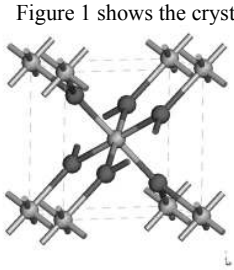

Figure 1. The unit cell of rutile TiO_2. Red spheres represent O atoms and light grey spheres represent Ti atoms.

First-principles calculations provide the methods that can be used to simulate a wide range of material properties. For many years, the local-density approximation (LDA) and generalized gradient approximations (GGA) within density functional theory (DFT) provided an efficient method for such calculations in solids, giving both lattice constants and bulk moduli with reasonable accuracy [1]. However, even though LDA and GGA gives acceptable crystal structures and ground state properties, it has the well-known band gap errors [8-11]. A more accurate description of the electronic structures is required. In this paper, we use a non-local exchange-correlation functional, the screened exchanged (sX) method [12], in order to correct the size of band gap and to improve the computational accuracy for TiO_2.

METHOD

The sX method is based on the Hartree-Fock method for the exchange potential energy that is separated into two terms. One term is Thomas-Fermi screened-exchange potential, and the other is the remainder. The remainder and correlation potential energy can be calculated by the LDA, while the Thomas-Fermi screened-exchange potential can be evaluated from:

$$V_C^{sX-LDA}(r,r') = -\sum_i \frac{\phi_i(r) exp-(k_{TF}|r-r'|)\phi_j^*(r)}{|r-r'|} \quad (1)$$

In Equation (1), V_C^{sX-LDA} is the non-local screened-exchange potential energy, ϕ are the Kohn-Sham orbitals, and k_{TF} is the Thomas-Fermi screening wave vector. The exchange-correlation hole can be calculated in an accurate way by using the Thomas-Fermi screening of the Hatree-Fock exchange potential energy, so it is consequently become non-localized electrons system compare with the LDA. Moreover, sX modified the non-existing discontinuity errors of exchange- correlation potential from LDA. Thus, the sX method improves the simulation accuracy for the value of energy band gap and has been found to give good results for some semiconductors and insulators.

In this work, we constructed a 2x2x2 supercell of 48 atoms of rutile TiO_2, containing a single oxygen vacancy or titanium interstitial. The oxygen vacancy is created by taking out one oxygen atom from the supercell; and similarly, an extra titanium atom is placed into the supercell to form the titanium interstitial model. The defect structures are relaxed in their various charge states by sX functional using the standard norm-conserving pseudopotentials, and the energy levels and density of states are then obtained through the optimized structures. Cut-off energy 750 eV was used which was decided by the energy convergence test. For the k- point integration, we specified at Γ point. A Γ k-point selection indicates that the calculation is doing at a single k-point (0,0,0) in the Brillouin zone.

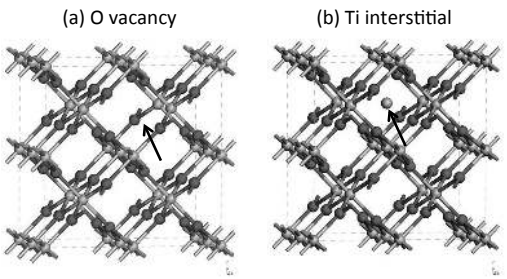

Figure 2. The crystal structures for rutile TiO_2 of (a) O vacancy, and (b) Ti interstitial. The defect sites are indicated by the arrows.

RESULTS

The band structure calculated by sX is shown in Figure 3, and Table 1 compares the calculated band gaps of rutile TiO_2 between sX, GGA and the experiment value. It can be seen that the band gap improves significantly from 1.86 eV in GGA to 3.1 eV in sX. The sX gap is close to experiment now. It is often thought that the band gap error is about 30%. This is true for Si, but for some oxides such as TCOs the error can be closer to 70-80% [13]. For rutile TiO_2, the gap opens up by 40% from GGA to sX in our calculations.

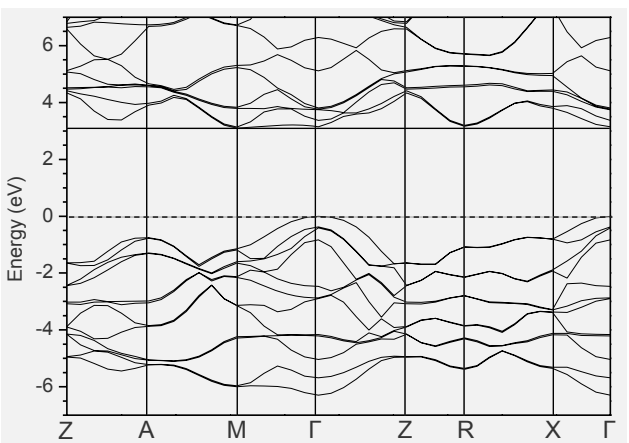

Figure 3. Band structure of rutile TiO_2 using the sX method. The red horizontal line marks the size of the band gap.

TiO_2 rutile	GGA	sX	Experiment
Band gap (eV)	1.86	3.1	3.1
Lattice constant (a/c) (Å)	4.64 / 2.97	4.56 / 2.98	2.59 / 2.96

Table 1. The band gaps and lattice constants calculated by the GGA and sX compared to the experimental value for rutile TiO_2.

Regarding the oxygen deficient, we consider firstly the oxygen vacancy of TiO_2. In this paper, we denote V_O^0, V_O^+ and V_O^{2+} for neutral, singly charged and doubly charged states respectively. The partial density of states (PDOS) calculated by sX were given in Figure 4. It reveals a defect level which is indicated by the arrow in the figure for V_O^0 and V_O^+. The position of the defect level is around 0.6 eV under the conduction band (CB) edge, agrees very well with experimental value [14]. There is no gap state for V_O^{2+}, because the excess electrons at the vacancy site would be neutralized by the doubly positive charge. The sX method gives a correct description of the localization of defect charge densities, which is not the case for the GGA [3-6].

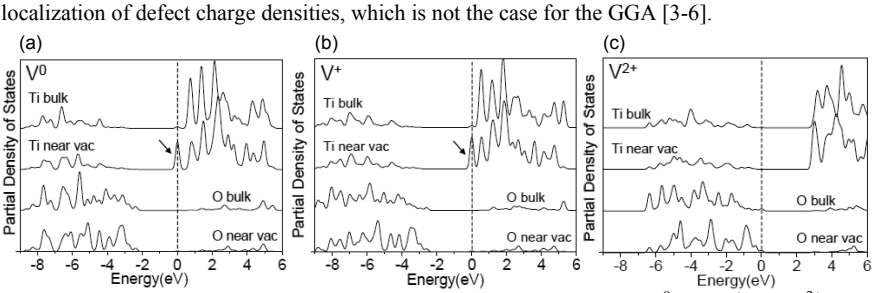

Figure 4. PDOS of O vacancy for rutile TiO_2 using the sX method, (a) V_O^0 (b) V_O^+ (c) V_O^{2+}.

Figure 5 shows a charge density contour for V_O^0 and V_O^+ of rutile TiO_2. The two excess electrons are located on two of three titanium atoms next to the oxygen vacancy site. The singly positive oxygen vacancy has an unpaired electron which is localized around the two titanium atoms close to the oxygen vacancy site.

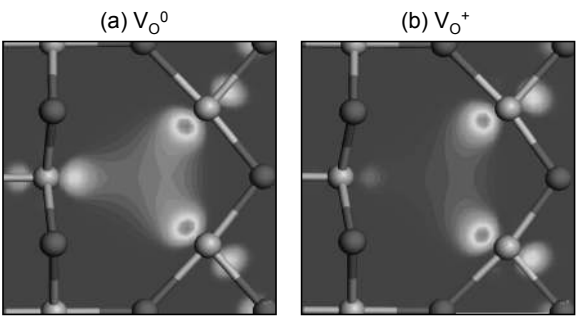

Figure 5. Charge density contour for the O vacancy site of rutile TiO_2, (a) V_O^0 (b) V_O^+, using sX method.

In the case of titanium interstitial, the DOS of Ti_i^0 is given in Figure 6.

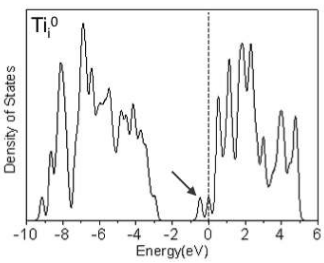

Figure 6. DOS of Ti interstitial neutral state (Ti_i^0) for rutile TiO_2 using the sX method.

Figure 7 shows the oxygen vacancy and titanium interstitial formation energy as a function of Fermi energy. In this figure, the red lines represent the oxygen vacancy and the black lines are the titanium interstitial which were both calculated by the sX method. It is found that the defect formation energies, for the neutral charge state, of oxygen vacancy and titanium interstitial are quite similar, 2.40 eV and 2.45 eV respectively, for an oxygen chemical potential in the O-poor condition. The similar size of these two calculated energies indicates that both are a cause of oxygen deficiency. The transition energy of the oxygen vacancy lies within the band gap, corresponds to the electrons trapped at adjacent titanium sites.

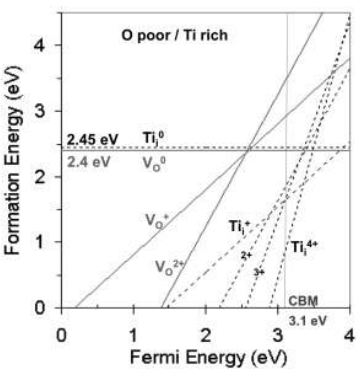

Figure 7. Formation energy against Fermi energy of the O vacancy and Ti interstitial in rutile TiO_2, calculated by sX.

CONCLUSIONS

This study presents an accurate band gap 3.1 eV for rutile TiO_2 by the sX exchange-correlation functional in DFT. The oxygen vacancy and titanium interstitial both create defect levels inside the band gap, and they are both a cause of oxygen deficiency according to their similar formation energy levels.

REFERENCES

1. S. J. Clark and J. Robertson, *Phys. Rev. B* **82**, 085208 (2010).
2. S. Wendt et al, *Science* **320**, 1755 (2008).
3. B. J. Morgan and G.W. Watson, *Surface Sci* **601**, 5034 (2007).
4. B. J. Morgan and G.W. Watson, *Phys. Rev. B* **80**, 233102 (2009).
5. C. DiValentin, G. Pacchioni and A. Selloni, *J. Phys. Chem. C* **113**, 20543 (2009).
6. S. Lany and A. Zunger, *Phys. Rev. B* **80**, 085202 (2009).
7. U. Diebold, *Surf. Sci. Rep.* **48**, 53 (2003).
8. S. J. Clark and J. Robertson, *Phys. Status Solidi B* **248**, 537 (2011).
9. L. J. Sham and M. Schluter, *Phys. Rev. Lett.* **51**, 1888 (1983).
10. J. P. Perdew and M. Levy, *Phys. Rev. Lett.* **51**, 1884 (1983).
11. R. W. Godby, M. Schluter and L. J. Sham, *Phys. Rev. Lett.* **56**, 2415 (1986).
12. D. M. Bylander and L. Kleinman, *Phys. Rev. B* **41**, 7868 (1990).
13. J. Robertson, K. Xiong and S. J. Clark, *Phys. Status Solidi B* **243**, 2054 (2006).
14. V. E. Henrich, G. Dresselhaus and H. J. Zeiger, *Phys. Rev. Lett.* **36**, 1335 (1976).

Mater. Res. Soc. Symp. Proc. Vol. 1352 © 2011 Materials Research Society
DOI: 10.1557/opl.2011.1079

Synergistic effects on band gap-narrowing in titania by doping from first-principles calculations: density functional theory studies

Run Long[1] and Niall J. English[1]
[1]The SEC Strategic Research Cluster and the Centre for Synthesis and Chemical Biology, Conway Institute of Biomolecular and Biomedical Research, School of Chemical and Bioprocess Engineering, University College Dublin, Belfield, Dublin 4, Ireland

ABSTRACT

The large intrinsic band gap in TiO_2 has hindered severely its potential application for visible-light irradiation. We have used a passivated approach to modify the band edges of anatase-TiO_2 by codoping of X (N, C) with transition metals (TM=W, Re, Os) to extend the absorption edge to longer visible-light wavelengths. It was found that all the codoped systems can narrow the band gap significantly; in particular, (N+W)-codoped systems could serve as remarkably better photocatalysts with both narrowing of the band gap and relatively smaller formation energies and larger binding energies than those of (C+TM) and (N+TM)-codoped systems. Our theoretical calculations help to rationalise experimental results and provide reasonably meaningful guides for experiment to develop more powerful visible-light photocatalysts.

INTRODUCTION

Titania (TiO_2)-based photocatalysts have received intense attention as promising photocatalytic materials [1]. However, their universal use is restricted to ultraviolent light ($\lambda <$ 385 nm) due to the wide band gap of titania (~3.2 eV for anatase). Further, photoexcited electron-hole pairs tend to recombine relatively easily in TiO_2. It is highly desirable to extend the optical absorption of TiO_2-based materials to the visible-light region with the minimum of photo-generated electron-hole recombination.

In general, doping is one of the most effective approaches to extend the absorption edge to the visible-light range. For instance, N-doped TiO_2 is considered to be a promising photocatalyst, and it has been investigated widely, both experimentally and theoretically [2]. However, due to strongly localized N 2p states at the top of valence band [3], the photocatalytic efficiency of N-doped TiO_2 decreases because isolated empty states trap an appreciable proportion of photo-excited electrons and reduce photo-generated current [4]. Besides N-doped TiO_2, C-doped TiO_2 also shows photocatalytic activity under visible-light [5].Conversely, transition metal doping can also promote photocatalytic efficiency, but this is hindered by the presence of carrier recombination centers and the formation of strongly localized d states in the band gap, which serves to reduce carrier mobility substantially [6]. Recently, Gai et al. [7] proposed using a passivated codoping approach, consisting of nonmetal and metal elements, to extend the TiO_2 absorption edge into the visible light range. Because defect bands are passivated, it is highly likely that they will be less effective as carrier recombination centers [8]. Recent experiments have reported that the addition of W to N-doped TiO_2 can increase photocatalytic activity under visible-light irradiation significantly [9, 10]. Our theoretical calculations on (N+W)-codoped

anatase suggest that a continuum band is formed at the top of the valence band, and that W 5d orbitals locate below Ti 3d states at the bottom of conduction band, which narrows significantly the band gap and enhances visible light absorption [11].

THEORY

Spin-polarized DFT calculations were performed using the projector augmented wave (PAW) pseudopotentials as implemented in the Vienna ab initio Simulation Package (VASP) code [12, 13]. The Perdew and Wang parameterization [14] of the generalized gradient approximation (GGA) [15] was adopted for exchange-correlation. The electron wave function was expanded in plane waves up to a cutoff energy of 400 eV and a Monkhorst–Pack *k*-point mesh [16] of $4 \times 4 \times 4$ was used for geometry optimization [17, 18] and electronic property calculations. Both the atomic positions and cell parameters were optimized until residual forces were below 0.01 eV/Å. It is well known that GGA underestimates the band gap of TiO_2 significantly (2.0 eV vs. anatase 3.2 eV experimental value). Here, we include the on-site Coulomb correction for the Ti 3d states, the GGA + U method [19], which can improve the prediction of the band gap. Here, U = 5.3 eV for Ti, which is in agreement with the optimal value (5.5±0.5eV) [20, 21]; using this, the calculated band gap of pure anatase was 3.11 eV, agreeing well with the experimental value of 3.20 eV. A variety of U values (1.0, 2.0, 3.0, and 4.0 eV) were applied to the dopants. The calculated results for U=1.0 and 2.0 eV gave a qualitatively wrong metallic ground state as in the standard GGA calculations for W, and Os, and the once the U value was increased to 3.0 eV, the behavior of W- and Os-doped TiO_2 exhibited appropriate semiconductor characteristics. For Re-doped TiO_2, the band gap is not particularly dependent on the U value. Therefore, a moderate value of U = 3.0 eV has been applied to TM 5d states, similar to V-doped TiO_2 [22].

A relaxed $(2 \times 2 \times 1)$ 48-atom anatase supercell was used to construct doped systems. Single O and Ti atoms were replaced by single X (N, C) and TM (W, Re, Os) atoms, respectively. The codoped systems were created by simultaneous substitution of an O atom by an X (N, C) atom and a Ti atom by a TM (W, Re, Os) atom. In principle, the three 5d transition metal elements W, Re and Os served as n-type dopants and non-metal elements N, C as p-type dopants. It was found that formation of adjacent metal-nonmetal element pairs is more energetically favorable with respect to other configurations. For clarity, we have listed the total energies differences between X-TM nearest-neighbor (*1nn*), the second nearest-neighbor (*2nn*) and largest-distance (*Lnn*, one dopant in the center of the supercell with the other in a corner) doped systems in Table 1. Here we set the *1nn* total energies as zero eV. We will select the lowest-energy structures to examine their electronic properties.

Table 1. Total energy difference of different doping systems (in eV). The total energy of nearest-neighbor configuration (*1nn*) has been set as zero.

	N+W	**N+Re**	**N+Os**	**C+W**	**N+Re**	**C+Os**
1nn	*0*	*0*	*0*	*0*	*0*	*0*
2nn	*0.48*	*0.95*	*1.0*	*1.1*	*0.35*	*3.1*
Lnn	*0.57*	*1.1*	*1.1*	*1.3*	*0.56*	*3.3*

DISCUSSION

We propose to codope anatase with donor-acceptor pairs to reduce the formation energy and to narrow the band gap further. Therefore, we calculated the formation energy for (X+TM)-codoped system, *i.e.* (N+W), (N+Re), (N+Os), (C+W), (C+Re), and (C+Os), according to

$$E_{form} = E(TM@Ti + X@O) - E(TiO_2) - \mu_X - \mu_{TM} + \mu_O + \mu_{Ti} \quad (1)$$

where $E(TM@Ti + X@O)$ is the total energy of the codoped system. The formation energies are also summarized in Table 1. The results show that codoping of X (N, C) with TM (W, Re, Os) reduces the formation energies significantly with respect to N and C monodoping under O-rich conditions, which corresponds to the usual growth conditions for synthesis samples in experiments. This indicates that codoping is beneficial for C or N introduction into the titania lattice. Hence, one could select W, Re, and Os to act as the codopants with N or C to favor the incorporation of N or C into the titania lattice in experiments. Furthermore, (N+TM)-codoped systems have lower formation energies than (C+TM)-doped TiO_2, which means that synthesis of the (N+TM) samples is relatively easier than the (C+TM) case.

Before we study the passivation effect on the band gap of TiO_2 via X-TM codoping, one needs to consider the stability of defect pairs. Therefore, we calculated the defect pair binding energy [33] according to

$$E_b = E(TM@Ti) + E(C@O) - E(TM@Ti + C@O) - E(TiO_2) \quad (2)$$

$$E_b = E(TM@Ti) + E(N@O) - E(TM@Ti + N@O) - E(TiO_2) \quad (3)$$

Positive E_b values indicate that the defect pairs tend to bind to each other and are stable. The calculated binding energies for the (C+W), (C+Re), (C+Os), (N+W), (N+Re), and (N+Os) pairs are 3.15, 0.65, 3.94, 2.64, 0.23, and 2.54 eV, respectively, indicating that C-W, C-Os, N-W, and N-Os impurities pairs are significantly stable relative to the isolated dopants. Furthermore, these binding energies are comparable with the reported result of Gai et al. [7]. However, the values of binding energy for C-Re and N-Re impurities pairs are not large enough and may possibly be broken up at high temperatures during the synthesis process. To confirm this, we also calculated the binding energies with a 108-atom supercell using a $2 \times 2 \times 2$ *k*-mesh. The corresponding values are 2.84, 0.50, 4.56, 2.28, 0.20, and 2.55 eV, respectively, indicating that the binding energies from the 48-atom system is reasonable. The large binding energy results arises from charge transfer from donor to acceptor and the strong associated Coulomb interaction is due to interactions between positively charged donors and negatively charged acceptors. The ELF is plotted in Fig. 1 at the (100) surface of bulk anatase for these three doped systems and the Bader charges are summarized in Tables 2 and 3 [34, 35]. Here, the partial optimized geometries are presented in Fig. 2 to compare with Tables 2 and 3. Fig. 1 shows that C-W and C-Re bonds exhibit ionic behavior while C-Os shows covalent characteristics. Table 2 shows that the C ion has a charge of -1.20 |e| for C@O monodoping, while it is -2.60 |e| for (C+W)-codoping, with more electrons transferring from the W and adjacent Ti atoms to the C ion. The bond length of C-W is 1.868 Å, which is shorter than that of the C-Ti length of 2.196 Å for C@O doping, indicating further that a strong C-W bond forms. For (C+Re), the optimized C-Re bond length is only 1.624 Å, shorter than that of C-W and significantly shorter than that of C-Ti. Therefore, a much stronger interaction between the C and Re ion takes place. For the (C+Os) system, the C-